



**University of
Zurich**^{UZH}

**Zurich Open Repository and
Archive**

University of Zurich
University Library
Strickhofstrasse 39
CH-8057 Zurich
www.zora.uzh.ch

Year: 2018

Morphological characterization of basally located uninucleate trophoblast cells as precursors of bovine binucleate trophoblast giant cells

Attiger, Jeannette ; Boos, Alois ; Klisch, Karl

Abstract: Binucleate trophoblast giant cells (TGCs) are one characteristic feature of the ruminant placenta. In cows, the frequency of TGCs remains constant for most of the duration of pregnancy. As TGCs are depleted by their fusion with uterine epithelial cells, they need to be constantly formed. It is still unclear whether they develop from stem cells within the trophoderm or whether they can arise from any uninucleate trophoblast cell (UTC). Within the latter, generally accepted theory, a basally located uninucleate cell (BUC) without contact to the fetomaternal interface would represent a transient cell between a UTC and a TGC. So far, no evidence for the existence of such transient cells or for the presence of stem cells has been shown. The aim of the present study is to morphologically characterize the early stages of TGC development. Placental tissue of 6 pregnant cows from different gestational stages (gestational days 51-214) was examined for BUCs, UTCs, and TGCs either in serial sections (light and transmission electron microscopy, TEM, n = 3), in single sections (TEM, n = 2), or by serial block face-scanning electron microscopy (n = 1). These investigations revealed the occurrence of BUCs, as well as young TGCs showing contact with the basement membrane (BM), but without apical contact to the fetomaternal interface. The study morphologically defines these 2 cell types as early stages of TGC development and shows that binucleation of TGCs can precede detachment from the BM.

DOI: <https://doi.org/10.1159/000489257>

Posted at the Zurich Open Repository and Archive, University of Zurich

ZORA URL: <https://doi.org/10.5167/uzh-159052>

Journal Article

Published Version

Originally published at:

Attiger, Jeannette; Boos, Alois; Klisch, Karl (2018). Morphological characterization of basally located uninucleate trophoblast cells as precursors of bovine binucleate trophoblast giant cells. *Cells, Tissues, Organs*, 205(3):151-163.

DOI: <https://doi.org/10.1159/000489257>

Morphological Characterization of Basally Located Uninucleate Trophoblast Cells as Precursors of Bovine Binucleate Trophoblast Giant Cells

Jeannette Attiger Alois Boos Karl Klisch

Institute of Veterinary Anatomy, University of Zurich, Zurich, Switzerland

Keywords

Placenta · Pregnancy · Cattle · Trophoblast giant cells · Stem cells

Abstract

Binucleate trophoblast giant cells (TGCs) are one characteristic feature of the ruminant placenta. In cows, the frequency of TGCs remains constant for most of the duration of pregnancy. As TGCs are depleted by their fusion with uterine epithelial cells, they need to be constantly formed. It is still unclear whether they develop from stem cells within the trophoderm or whether they can arise from any uninucleate trophoblast cell (UTC). Within the latter, generally accepted theory, a basally located uninucleate cell (BUC) without contact to the fetomaternal interface would represent a transient cell between a UTC and a TGC. So far, no evidence for the existence of such transient cells or for the presence of stem cells has been shown. The aim of the present study is to morphologically characterize the early stages of TGC development. Placentomal tissue of 6 pregnant cows from different gestational stages (gestational days 51–214) was examined for BUCs, UTCs, and TGCs either in serial sections (light and transmission electron microscopy, TEM, $n = 3$), in

single sections (TEM, $n = 2$), or by serial block face-scanning electron microscopy ($n = 1$). These investigations revealed the occurrence of BUCs, as well as young TGCs showing contact with the basement membrane (BM), but without apical contact to the fetomaternal interface. The study morphologically defines these 2 cell types as early stages of TGC development and shows that binucleation of TGCs can precede detachment from the BM.

© 2018 S. Karger AG, Basel

Abbreviations used in this paper

BM	basement membrane
BUC	basally located uninucleate cell
DLB	double lamellar body
EMT	epithelial-mesenchymal transition
gd	gestational day
LM	light microscopy
PL	placental lactogen
rER	rough endoplasmic reticulum
SBF-SEM	serial block face-scanning electron microscopy
TEM	transmission electron microscopy
TGCs	trophoblast giant cells
TNV	total nuclear volume
UTCs	uninucleate trophoblast cells

Introduction

The trophoblast epithelium of the bovine placenta consists of uninucleate trophoblast cells (UTCs) and trophoblast giant cells (TGCs), also called binucleate trophoblast cells, BNCs [Björkmann, 1969; Klisch et al., 1999a, b]. These 2 cell types are characteristic elements of the ruminant fetal placenta [Hoffman and Wooding, 1993; Wooding and Burton, 2008] with a morphology that is largely uniform within the different ruminant species [Wooding, 1992].

UTCs show a cuboidal to columnar shape [Wathes and Wooding, 1980], have contact to the trophoctodermal basement membrane (BM) [Wimsatt, 1951], and their microvilli interdigitate with those of the uterine epithelial cells [Björkmann, 1969; Wathes and Wooding, 1980]. The cytoplasm shows polysomes, rough endoplasmic reticulum (rER), and a small Golgi apparatus. Their numerous mitochondria are located in the apical part of the cell, while lipid droplets and vesicles of different size are situated near the BM [Björkmann, 1969; King et al., 1980].

TGCs are migrating cells, which develop in the basal part of the trophoblast epithelium [Wimsatt, 1951; Morgan and Wooding, 1983] and move apically to the fetomaternal contact zone to fuse with the uterine epithelium [Wathes and Wooding, 1980; Wooding and Wathes, 1980; Wooding, 1983]. Young, basally located TGCs [Wimsatt, 1951; Morgan and Wooding, 1983] do not have contact to the BM or to the fetomaternal border [Hoffman and Wooding, 1993]. They possess a rounded shape and show a great amount of cytoplasmic ribosomes [Björkmann, 1968; Wooding, 1992]. Mature, apically migrating TGCs have an increased cell as well as nuclear volume [Morgan and Wooding, 1983; Wooding, 1992; Klisch et al., 1999b] and show numerous small mitochondria, plenty of rER, and a large Golgi apparatus [Björkmann, 1968; Morgan and Wooding, 1983; Wooding, 1992]. They contain a remarkable amount of membrane-bound granules, which incorporate a variety of secretory proteins [Wooding and Beckers, 1987; Zoli et al., 1992; Klisch and Leiser, 2003]. Additionally, they possess a special organelle called a double lamellar body (DLB), which has been claimed to be characteristic for TGCs while its function has not been described yet [Wooding and Burton, 2008].

The production of the cytoplasmic membrane-bound granules, which contain placental lactogen (PL) [Wooding and Beckers, 1987], prolactin-related protein-I [Klisch and Leiser, 2003], and pregnancy-associated glycoproteins [Zoli et al., 1992; Klisch and Leiser, 2003], displays an important function of TGCs. In cattle, the fusion of a

TGC with a uterine epithelial cell forms a fetomaternal hybrid cell, which delivers the content of the cytoplasmic granules to the maternal tissue and circulation by basal exocytosis [Wathes and Wooding, 1980; Wooding, 1983; Wango et al., 1990]. As the fetomaternal hybrid cell degenerates after having transferred the content of the granules into the maternal tissue [Wooding and Wathes, 1980; Hoffman and Wooding, 1993], this protein delivery process implies a reduction of TGC number in the fetal tissue. However, their fraction within the trophoctoderm is relatively consistent at about 20% until the end of gestation [Wooding and Wathes, 1980]. Thus, a constant production of TGCs during pregnancy is required.

The origin of TGCs has been discussed by different authors, but is still not fully clarified. Wimsatt [1951] identified mature TGCs as “postmitotic” cells due to the absence of cleavage-furrows in any TGC. He described the development of these cells by transforming UTCs, which acquire a round shape, lose contact to the BM, and become binucleate by acytokinetic mitosis [Wimsatt, 1951].

Greenstein et al. [1958] described an undifferentiated, polygonal to cuboidal cell type in the peri-implantational trophoctoderm, which they construed to be a stem cell for both UTCs and TGCs [Greenstein et al., 1958]. The most recent and widely accepted theory about the origin of TGCs has been established by Wooding and his colleagues [Wooding, 1992; Wooding and Burton, 2008]. They suggest that any typical UTC can perform an asymmetric mitosis. One daughter cell of this mitosis is a basally located uninucleate cell (BUC), which subsequently develops into a TGC by losing contact to the BM and becoming binuclear by an acytokinetic mitosis.

Despite these concepts being frequently referred to [Klisch et al., 1999a, b; Klisch and Leiser, 2003; Igwebuike, 2006; Haeger et al., 2016], to our knowledge, no evidentiary images for the existence of such a basally located uninucleate transient or stem cell in the mature bovine placenta have been published. Thus, the aim of this study is to verify the existence of BUCs and to characterize the early stages of TGC development in cows morphologically. To settle these questions, amongst others, an automated serial sectioning technique (serial block face-scanning electron microscopy, SBF-SEM), will be used.

Materials and Methods

Tissue Preparation

Placental tissue was collected from 6 pregnant cows (gestational day, gd, 51, 109, 120, 140, 158, and 214) at a local slaughterhouse. Uteri were obtained approximately 30 min after the death of the

cow by bolt shot and exsanguination. The gestational stage was estimated based on the measured fetal crown-rump length [Schnorr and Kressin, 2011].

Tissue from 5 of these cows (gd 51, 109, 120, 140, 214) was prepared for light microscopy (LM) and conventional transmission electron microscopy (TEM). One randomly chosen placentome was perfused with 20 mL of 2.5% glutaraldehyde in 0.1 M sodium/potassium (Na/K) phosphate buffer. For this perfusion, a fetal placental blood vessel close to the chosen placentome of the opened uterus was clipped with the tip of small scissors, a blunt 21-G butterfly winged cannula (B. Braun Venofix 21G Butterfly Winged Cannula Needles, B. Braun Melsungen AG, Melsungen, Germany) was introduced into the vessel and fixed with hemostats to the surrounding tissue to hold it in position. Then, perfusion was performed manually with soft pressure by a 20-mL syringe for 1–2 min without any prewashes. A slice of 1–2 mm thickness and ranging from the top to the bottom of the placentome was cut out centrally of the placentome with a sharp razorblade and was trimmed to cubes of 1–2 mm side lengths with the same razorblade. These cubes were immersed in the same fixative as used for perfusion for 1 h at 0–4 °C. After fixation, the tissue was stored in cold 0.1 M Na/K phosphate buffer until it was postfixed with 1% osmium tetroxide in 0.1 M Na/K phosphate buffer, dehydrated in a graded series of ethanol and embedded in epon. If necessary, the tissue cubes were trimmed to side lengths of 1 mm before postfixation.

For SBF-SEM, 1 placentome of a pregnant cow (gd 158) was perfused with 20 mL of 2.5% glutaraldehyde and 2% formaldehyde in 0.15 M cacodylate buffer (pH 7.4) containing 2 mM of calcium chloride (CaCl₂). Perfusion was performed in the same way as perfusion of the tissue for LM and TEM. A slice of 1–2 mm thickness and ranging from the top to the bottom of the placentome was cut out centrally of the placentome with a sharp razorblade and was trimmed to cubes of 1–2 mm side lengths with the same razorblade. These cubes were immersed in the same fixative as used for perfusion for 3 h at 0–4 °C. Following fixation, the tissue was washed (4 × 3 min) in cold 0.15 M cacodylate buffer containing 2 mM of CaCl₂ on a shaker and then stored in fresh buffer at 4 °C until further processing. If necessary, the tissue cubes were trimmed to side lengths of 1 mm before they were further treated following a protocol optimized for SBF-SEM [Deerinck et al., 2010]. Tissue embedding was mainly performed as described in this protocol except for 2 modifications: using an epon mixture with a harder consistence (3.63 g epoxy embedding medium [Fluka, Sigma-Aldrich Chemistry GmbH, Buchs, Switzerland] + 2.63 g NMA [nadac methyl anhydride, Fluka, Sigma-Aldrich Chemistry GmbH] + 1.25 g DDSA [dodecyl succinic anhydride, Fluka, Sigma-Aldrich Chemistry GmbH] + 0.14 g DMP-30 [2,4,6-tris(dimethylaminomethyl)phenol, Fluka, Sigma-Aldrich Chemistry GmbH] for approximately 6 mL epon), which was polymerized at 60 °C for 2.5 days, and using Easy-Molds (EMS, Hatfield, PA, USA).

Serial Section Examination

Light Microscopy

Serial semithin sections (1 µm) were cut from tissue blocks of 3 animals (gd 51, 140, and 214) with an ultramicrotome (Ultracut E, Reichert, Vienna, Austria), mounted on glass slides (Menzel-Gläser, Braunschweig, Germany) and stained with toluidine blue. Alternating, sections were either coverslipped in Pertex (Medite, Burgdorf, Germany) or left without a coverslip. Within the series of covered sections, several cells were followed and photographed with a light

microscope. On the basis of the photographs, the cells were categorized into 3 groups: UTCs, which were light microscopically located on the BM and showed contact to the fetomaternal interface; TGCs, which exhibited 2 nuclei; or BUCs, which light microscopically did not show contact to the fetomaternal interface.

The nuclear volume of all examined cells was estimated according to the principle of Cavalieri [Mayhew, 1991] using Stereoinvestigator software (MBF Bioscience, Williston, VT, USA). In TGCs, the nuclear volumes of all nuclei in 1 cell were summed up as the total nuclear volume (TNV).

Transmission Electron Microscopy

From each series of semithin sections, 5 non-coverslipped sections, with a distance of 6 µm (5 sections) between each, were re-embedded in epon. This was performed according to the protocol described by Suzuki et al. [2003], while instead of BEEM capsules [Suzuki et al., 2003] Easy-Molds (EMS) were used. The re-embedded sections covered segments of the series where most of the light microscopically examined cells were located. After re-embedding, ultrathin sections (70 nm) were cut with an ultramicrotome (Ultracut E, Reichert), mounted on slot grids with formvar (EMS) or polystyrene 2,000,000 g/mol membrane (0.5 g of polystyrene solved in 100 mL chloroform) and stained with uranyl acetate and lead citrate. The cells examined by LM were followed within the ultrathin sections with a transmission electron microscope (CM12, Philips, Eindhoven, The Netherlands) and photographs were taken with a CCD camera (Ultrascan 1000 or Orius 832, Gatan, Pleasanton CA, USA). By means of the photographs, the cells were assessed regarding following criteria:

- contact to the BM
- contact to the fetomaternal interface
- presence of membrane-bound granules
- occurrence of particular organelles (DLB, mitochondria, and free cytoplasmic ribosomes in all 3 cell types, and Golgi apparatus and rER only in UTCs and BUCs)

In cases where none of the ultrathin sections of 1 semithin section were investigable due to rupture of the membrane or insufficient contrasting, an adjacent semithin section without coverslip was re-embedded, sectioned, and examined.

Statistical Methods

Statistical analysis of the estimated nuclear volumes was performed with SPSS 23 (IBM® SPSS® statistics, version 23.0, IBM Corp., USA).

Single Section Examination

Transmission Electron Microscopy

Ultrathin sections (70 nm) were cut from tissues of 2 animals (gd 109, 120) with an ultramicrotome (Ultracut E, Reichert), mounted on copper grids, and stained with uranyl acetate and lead citrate. In 6 sections of each animal, TGCs were observed with a transmission electron microscope (CM12, Philips) and photographs were taken with a CCD camera (Ultrascan 1000 or Orius 832, Gatan). All TGCs, which were visible in a total cross-section and showed 2 nuclei, were photographed. By means of the photographs, the cells were assessed regarding the following criteria:

- contact to the BM
- contact to the fetomaternal interface
- presence of membrane-bound granules
- occurrence of a DLB

Serial Block Face-Scanning Electron Microscopy

The prepared tissue of 1 animal (gd 158) was visualized in a SBF-SEM (FEI Quanta 250 FEG variable pressure SEM, Thermo Fischer Scientific) equipped with a Gatan 3View 2XP system and dedicated backscatter detector (Gatan). Two areas, which contained chorionic villi, were imaged with a voxel size of $11 \times 11 \times 100 \text{ nm}^3$. Images had $5,000 \times 5,000$ pixels and stacks of 1,000 images were produced.

The SBF-SEM images were edited with ImageJ (version 2.0.0-rc-43/1.51d, open source image processing software) as follows: inversion, smoothing, contrast enhancement of 0.5% and conversion from a 16-bit dm3-data file to an 8-bit tiff-data file. Image stacks were screened for BUCs, of which 1 cell was reconstructed to a three-dimensional image. Therefore, the selected cell was manually segmented with the ImageJ plugin TrakEM2. The cell nucleus, cell body, and the trophoblast epithelium were segmented separately in a stack of images and a three-dimensional model was created with Imaris x64 9.0.0 (Bitplane AG) software.

Results

Serial Section Examination

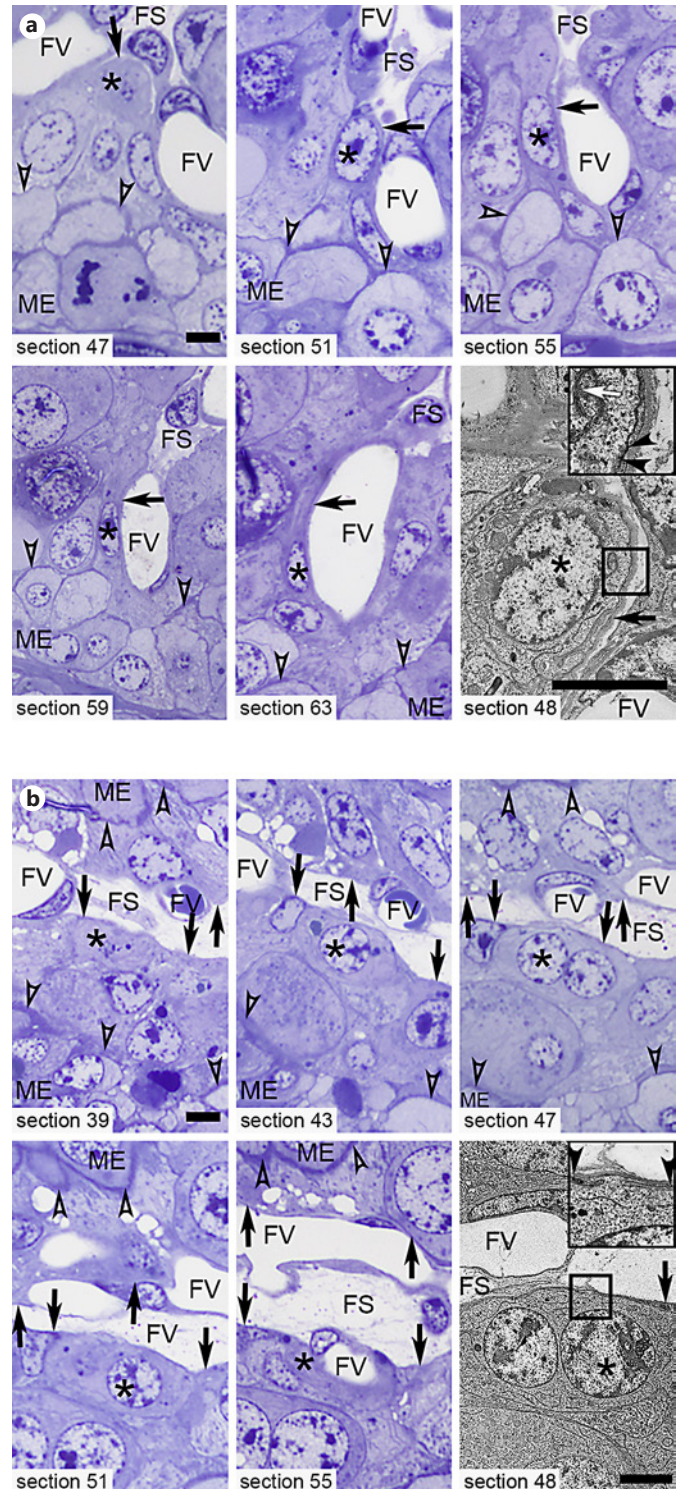
Light Microscopy

In the series of semithin sections, 63 TGCs, 20 BUCs, and 65 UTCs were followed (Fig. 1a, b) and their TNVs were determined. The TNVs of TGCs showed a wide variation and ranged from 491 to $2,777 \mu\text{m}^3$. TNVs of BUCs and UTCs showed both a unimodal distribution and ranged from 298 to $607 \mu\text{m}^3$ and from 161 to $679 \mu\text{m}^3$, respectively. All the measured TNVs are presented in histograms (Fig. 2a–c). The TNV of those cells which were examined by LM and TEM are also provided in the online supplementary Tables 1–3 (for all online suppl. material, see www.karger.com/doi/10.1159/000489257).

Fig. 1. Bovine trophoblast epithelium in serial sections of semithin sections in LM and an intermediate ultrathin section in TEM. FS, fetal stroma; FV, fetal vessel; ME, maternal epithelium. Scale bars, $5 \mu\text{m}$. **a** Serial sections of a BUC (asterisk) in LM (sections 47–63) with an intermediate TEM section (section 48). The TEM image of section 48 shows that the BUC has contact to the BM (black arrows, contact is shown between black arrowheads in the **inset** at a higher magnification) and a DBL (white arrow). No contact to the fetomaternal interface (open arrowheads) was visible in the examined semithin or ultrathin sections and the nuclear-cytoplasmic ratio seems, subjectively evaluated, to be rather high (gd 140). **b** Serial sections of a binucleate TGC (asterisk) in LM (sections 39–55) with an intermediate TEM section (section 48). This TGC shows contact to the BM (black arrows, contact is shown between black arrowheads in the **inset** at a higher magnification). No contact to the fetomaternal interface (open arrowheads) was visible in the examined semithin or ultrathin sections (gd 140).

Transmission Electron Microscopy

Since the morphological characteristics within each cell type did not show distinctions between the different gestational stages, cells from several animals are not de-



scribed separately. Some cells could not be unambiguously assigned to 1 cell type (TGC, BUC, or UTC) based on TEM. These cells, as well as the cells which could be examined on ultrathin sections from only 1 semithin section, were excluded from the ultrastructural evaluation. If the classification of the cell type differed between LM and TEM, the latter was regarded as valid.

Profiles of 32 TGCs were evaluated on ultrathin sections from 2 to 5 different semithin sections (online suppl. Table 1). In all 3 animals, TGCs with ($n = 11$) and without ($n = 17$) contact to the BM were visible. All TGCs with contact to the BM did not show contact to the fetomaternal interface (Fig. 3a, b) and only a few of them possessed membrane-bound granules (2 of 11) or a DLB (1

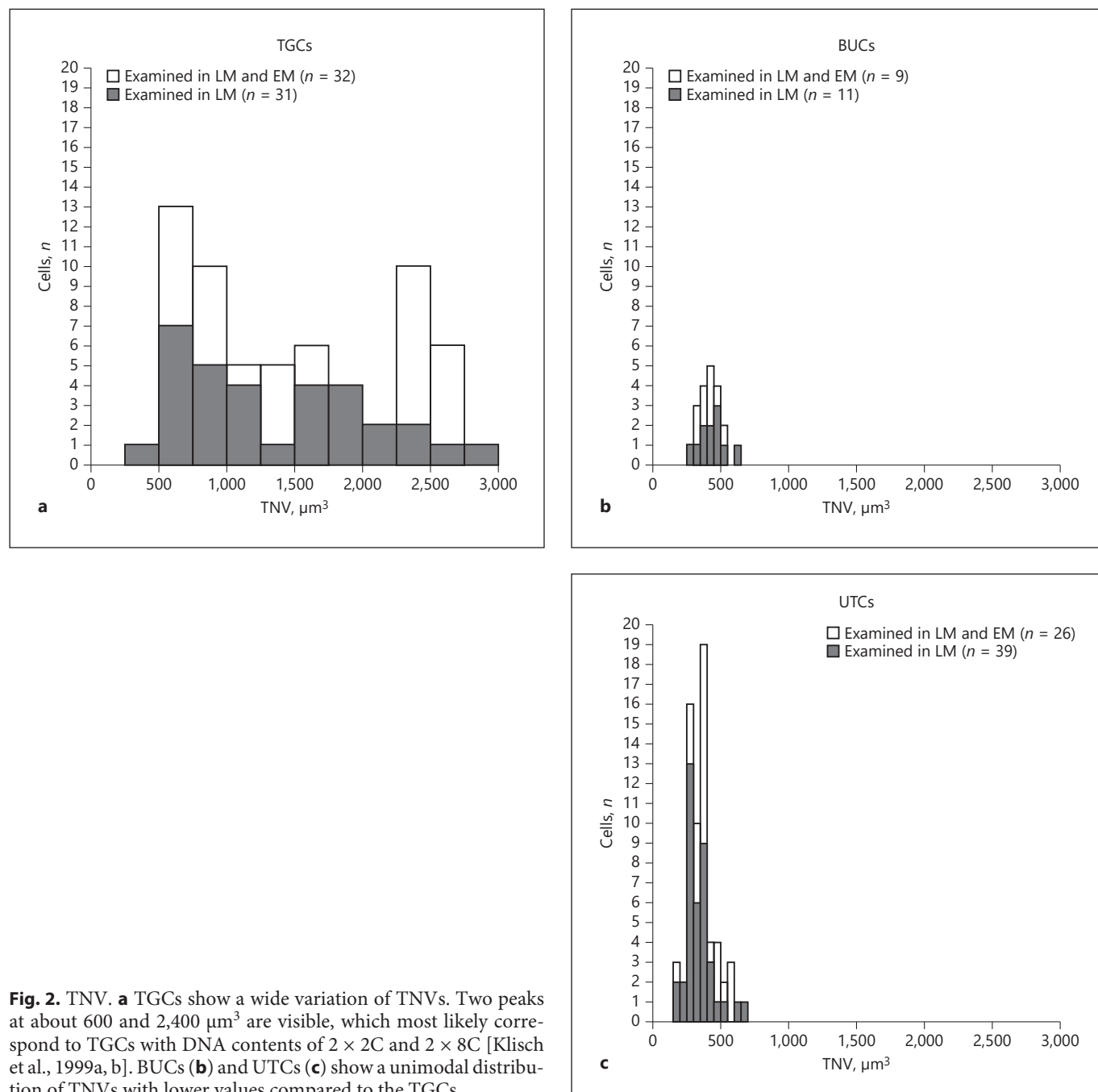


Fig. 2. TNV. **a** TGCs show a wide variation of TNVs. Two peaks at about 600 and 2,400 μm^3 are visible, which most likely correspond to TGCs with DNA contents of $2 \times 2C$ and $2 \times 8C$ [Klisch et al., 1999a, b]. BUCs (**b**) and UTCs (**c**) show a unimodal distribution of TNVs with lower values compared to the TGCs.

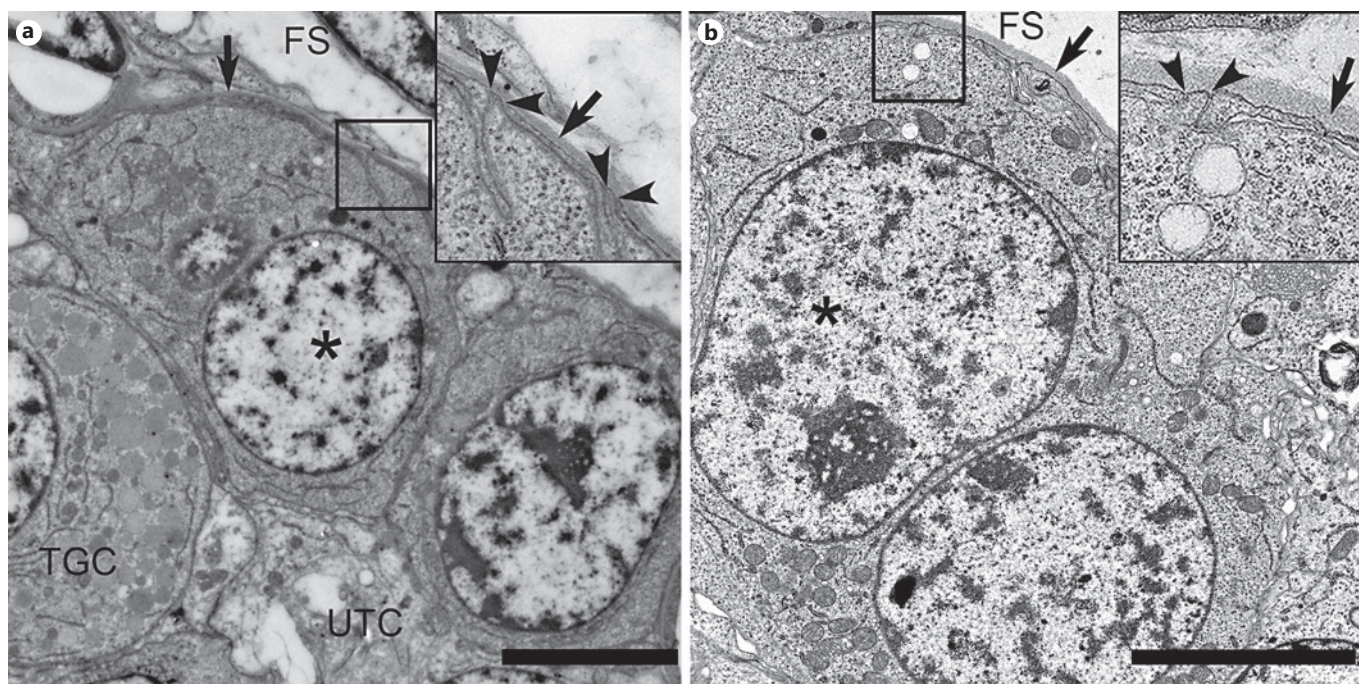


Fig. 3. TGCs (asterisk) with contact to the BM (black arrow, contact is shown between black arrowheads in the **inset** at a higher magnification). None of the TGCs with contact to the BM were in tangency to the feto-maternal interface. FS, fetal stroma. Scale bars, 5 μ m. **a** A binucleate TGC (asterisk) which reveals 2 narrow, tanged areas with contact to the BM (between the black arrowheads, gd 140). **b** A binucleate TGC (asterisk) which reveals a narrow, tanged contact to the BM (between the black arrowheads, gd 109).

of 11). The majority of the TGCs with contact to the BM showed, subjectively evaluated, a higher amount of free cytoplasmic ribosomes compared to UTCs (9 of 11) and mitochondria were diffusely distributed within the cytoplasm (10 of 11). Approximately half of the TGCs with contact to the BM showed a thin layer of electron-dense material associated with the inner surface of the cell membrane (5 of 11). This layer was either completely attached to the cell membrane, detached from the cell membrane in several places, or completely detached from the cell membrane, but surrounding the main part of the cytoplasmic organelles. TNVs of all TGCs with contact to the BM ranged from 588 to 1,326 μ m³.

The majority of TGCs without contact to the BM showed membrane-bound granules (12 of 17; Fig. 4a, b), diffusely distributed mitochondria (16 of 17), and, subjectively evaluated, a higher amount of free cytoplasmic ribosomes compared to UTCs (13 of 17). A DLB was observed in 3 out of 17 TGCs without contact to the BM. Most of these cells showed a layer of electron-dense material associated with the inner surface of the cell membrane as described above (16 of 17; Fig. 4a, b). This layer of elec-

tron-dense material was thicker compared to the one described in the TGCs with contact to the BM. In 2 TGCs without contact to the BM, contact to the feto-maternal interface was visible. The TNVs in all TGCs without contact to the BM varied between 508 and 2,671 μ m³.

In 4 TGCs without contact to the feto-maternal interface, the contact to the BM could not definitely be ruled out or confirmed, while their cytoplasmic content showed similarities to TGCs with and without contact to the BM. Their TNVs varied between 2,432 and 2,777 μ m³.

Ultrastructural details of 9 BUCs were evaluated on ultrathin sections from 2 to 4 different semithin sections (online suppl. Table 2). All of these BUCs showed contact to the BM but no contact to the maternal epithelium (Fig. 5a–d). A DLB was visible in 2 cells (Fig. 1a) and no cell showed cytoplasmic membrane-bound granules or a layer of electron-dense material, as found in the TGCs. The Golgi apparatus was not visible in any section of BUCs, and rER as well as mitochondria were rarely found in all examined BUCs. In most sections, where mitochondria were visible, they seemed to be diffusely distributed (in 8 of 9 BUCs). In 1 BUC, the amount of free cytoplas-

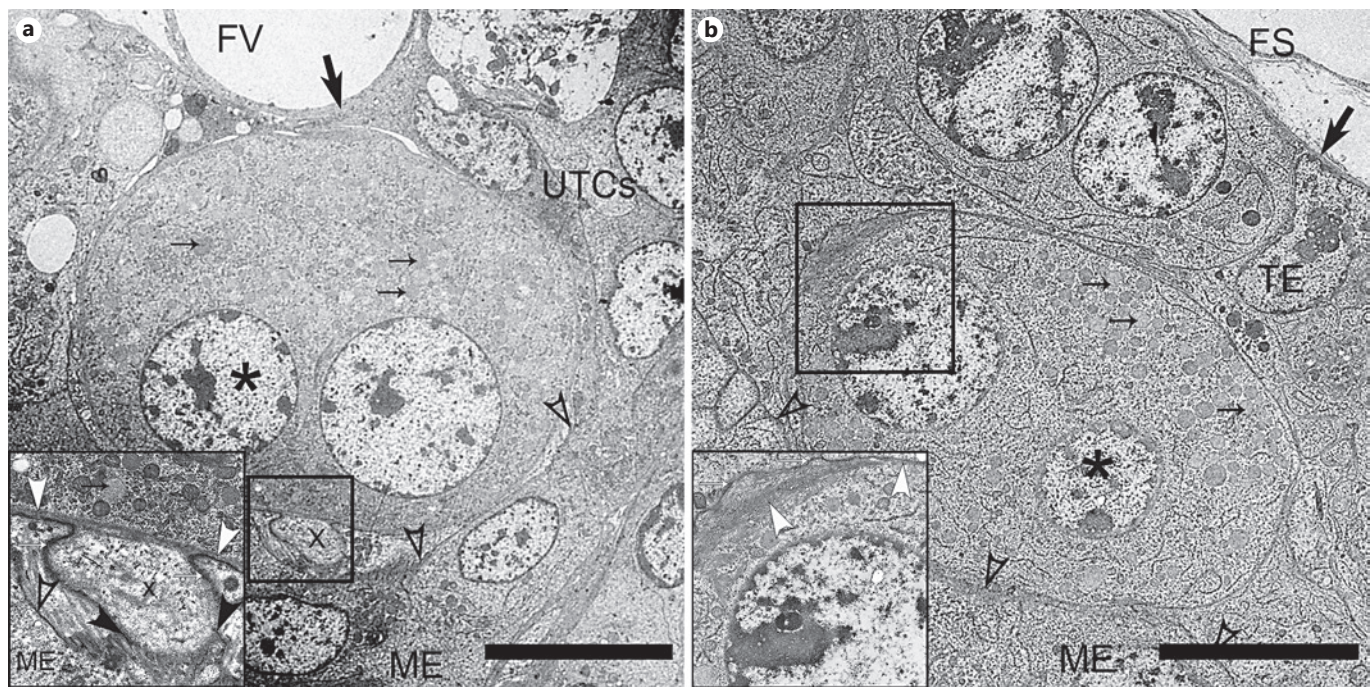


Fig. 4. Transmission electron microscopic sections of binucleate TGCs (asterisk) without contact to the BM (solid black arrow) and showing membrane bound granules (small black arrows) as well as intracellular electron-dense material attached to the cellular membrane (white arrowheads). The areas in boxes are shown at higher magnification in the **insets**. FS, fetal stroma; FV, fetal vessel; TE, trophoblast epithelium; open arrowheads, feto-maternal interface. Scale bars, 10 μ m. **a** A binucleate TGC showing an apical

protrusion (X), which is in contact with the maternal epithelium (ME). Along the inner surface of the cell membrane, a layer of electron-dense material (white arrowheads) is visible, which excludes the apical protrusion (shown in the **inset** at a higher magnification, gd 109). **b** A binucleate TGC close to the maternal epithelium (ME). A layer of electron-dense material (white arrowheads) is attached to the inner surface of the cell membrane (shown in the **inset** at a higher magnification, gd 140).

mic ribosomes was subjectively evaluated as higher compared to UTCs and, overall, the nuclear-cytoplasmic ratio, also subjectively evaluated, appeared to be rather high in BUCs (Fig. 1a, 5a–d).

The morphology of 26 UTCs was evaluated on sections from 2 to 4 different semithin sections (online suppl. Table 3). All examined UTCs had contact to the feto-maternal interface and did not show membrane-bound granules or a DLB. Contact to the BM was visible in 23 cells while it was not ($n = 1$) or unclearly ($n = 2$) represented in 3 cells. The distribution of mitochondria, which occurred in moderate amounts, varied between apical (12 of 26) and diffuse (14 of 26). In the majority of UTCs, electron-dense material was visible in the apical cell part within the region of the interdigitating microvilli, but no layer of electron-dense material was seen associated to the basolateral cell membrane (24 of 26, data not shown; online suppl. Table 3). A small Golgi apparatus was visible in 9 UTCs while a small amount of rER was seen in all UTCs.

Single Section Examination

Cross-sections of 62 binucleate TGCs were examined with TEM in single sections of 2 animals (online suppl. Table 4). In the majority of these cells, no contact to the BM was visible ($n = 55$; Fig. 4a, b). Most of the TGCs without contact to the BM possessed membrane-bound granules (50 of 55) and showed a layer of electron-dense material associated to the inner surface of the cell membrane as described in TGCs of serial sections (41 of 55; Fig. 4a, b). In 10 TGCs without contact to the BM, a DLB was visible and 4 of the TGCs without contact to the BM showed contact to the feto-maternal interface.

Narrow attachments to the BM were found in 4 TGCs. None of these 4 cells revealed contact to the feto-maternal interface, membrane-bound granules, or a DLB. The majority of TGCs with contact to the BM had a layer of electron-dense material associated to the inner surface of the cell membrane, as described in TGCs of serial sections (3 of 4). In 3 TGCs, the contact to the BM could not definitely be ruled out or confirmed, while none of them had

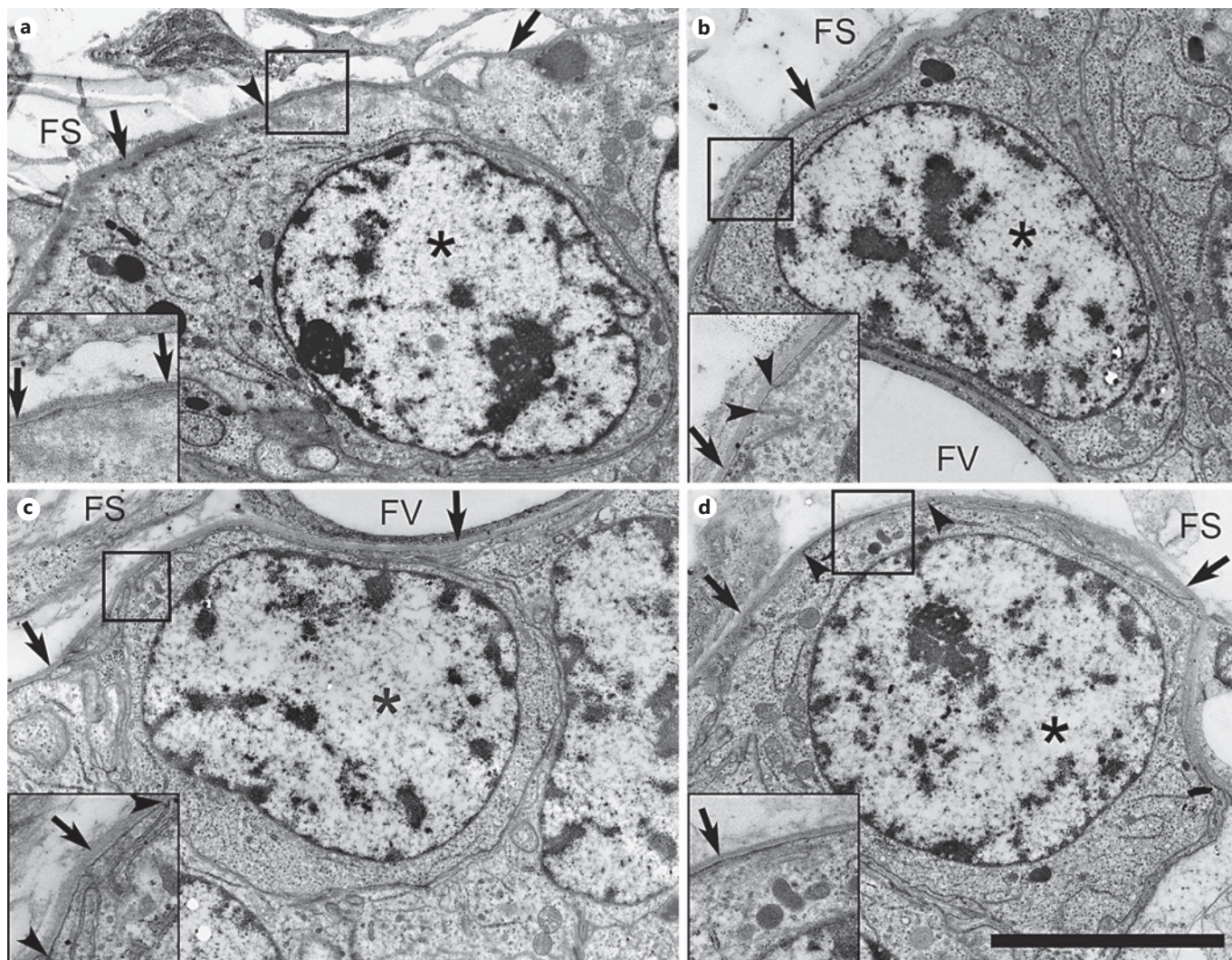


Fig. 5. Morphology of BUCs (asterisk) of the bovine trophoblast epithelium. Contact to the BM (black arrows), which was visible in all examined BUCs, is shown at a higher magnification in the **insets**. The nuclear-cytoplasmic ratio seemed, subjectively evaluated, to be rather high in BUCs. No examined BUC was in tangency

with the feto-maternal interface. FS, fetal stroma; FV, fetal vessel. Scale bar, 5 μ m. **a, d** A BUC with laminar contact to the BM (between the black arrowheads, gd 214 and 140). **b, c** A BUC with a petiolate contact to the BM (between the black arrowheads, gd 140).

contact to the feto-maternal interface or a DLB. Two of these cells possessed membrane-bound granules and 1 cell showed a layer of electron-dense material associated to the inner surface of the cell membrane, as described in TGCs of serial sections.

SBF-SEM

Within the images of SBF-SEM, 3 BUCs could be followed. These cells were located in the basal part of the trophoblast epithelium without contact to the maternal epithelium and possessed 1 nucleus. The three-dimen-

sional structure of 1 of these cells is presented in Figure 6a. Detailed ultrastructural morphology could not be examined due to an insufficient resolution (Fig. 6b).

Discussion

According to the currently generally accepted hypothesis about the origin of ruminant TGCs, a BUC would represent the direct progenitor for a TGC [Wooding, 1992; Wooding and Burton, 2008]. To the authors' knowl-

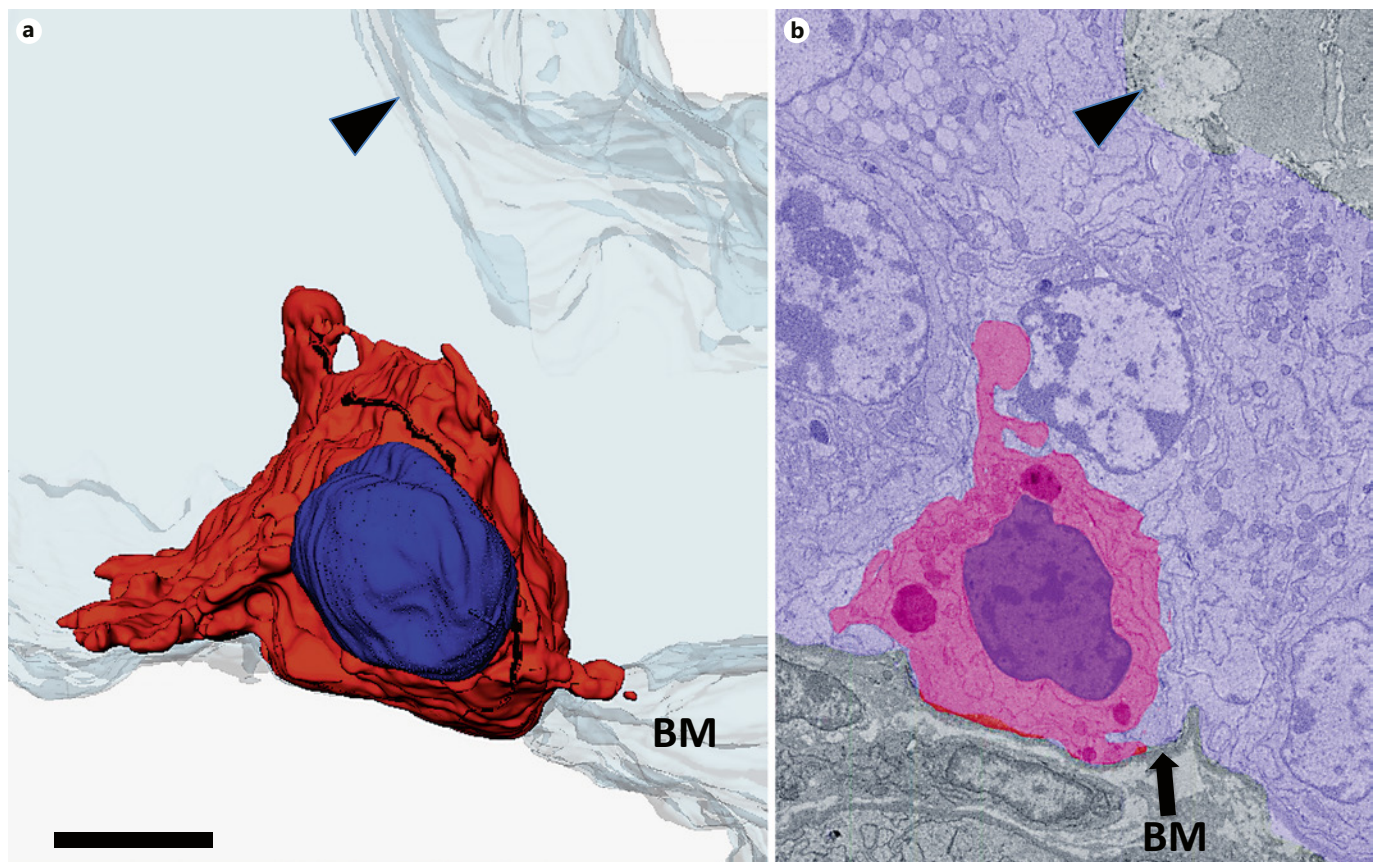


Fig. 6. **a** Three-dimensional model of a BUC, based on SBF-SEM images of the bovine trophoblast epithelium. The cell has several basal processes and is attached to the BM. No contact to the apical surface of the trophoblast epithelium (arrowhead) is present (gd 158). Scale bar, 5 μ m. **b** SBF-SEM image of the same cell.

edge, such a BUC has so far never been revealed. This is probably due to the difficulty of accessing three-dimensional information about individual cells from two-dimensional sections. In our study, we used 2 different methods to gain three-dimensional information. On the one hand, we performed manual serial sectioning in LM and TEM, which allowed us to evaluate the presence or absence of contact to the apical or basal epithelial surface, number of nuclei per cell, as well as nuclear volume and ultrastructural information about the cytoplasmic content. With this method, information between the examined sections, called the *z*-plane, became lost, while we obtained detailed information in the *xy*-plane by high resolution. On the other hand, we utilized a more modern technique, the SBF-SEM, which enabled us to reduce the loss of information in the *z*-plane (section thickness = 100 nm) compared to serial sectioning in TEM (distance between 2 examined sections = 6 μ m). Even though, as it was

necessary to view bigger areas containing chorionic villi, resolution in the *xy*-plane had to be reduced to restrict the running time of the SBF-SEM to a period of 62 h. For these reasons, SBF-SEM offered more complete information about the presence or absence of contact to the apical and basal epithelial surface and enabled a clear three-dimensional presentation of trophoblast epithelial cells, while cytoplasmic information was reduced. For both methods, tissue was perfused with fixative by a fetal placental vessel as the main interest was posed on the fetal trophoblast epithelium. Nevertheless, it is nicely visible on the images that the fetal epithelium and in particular the feto-maternal interface is well preserved without perfusion by a maternal placental vessel.

Even if the number of animals used in this study is relatively low, we consider the collected information as representative to answer the question posed in this study. This appears to be justified, first by the very de-

tailed information obtained by the 2 serial-sectioning methods used in this study and, second by the fact that there are no indications about major, gestational stage-dependent morphological variations within each trophoblast cell type from gd 45 until term [Björkmann, 1969], even though protein expression has been shown to vary within gestation [Green et al., 2000; Touzard et al., 2013].

A lack of contact to the BM is generally considered to be a distinctive feature of ruminant TGCs [Hoffman and Wooding, 1993; Wooding and Burton, 2008]. In our study, we showed for the first time that some binucleate TGCs still have narrow contact to the BM. Due to their basal location within the trophoblast epithelium and their relatively small TNVs, compared to all examined TGCs, we interpret these cells as early developmental stages of TGCs [Klisch et al., 1999b]. These results indicate that the process of losing basal contact does not have to be completed before the cells become binucleate. Findings of previous studies showed that alpha-keratin is localized in basally located binucleate cells, but not in mature, apically migrated cells [Lee et al., 1990]. This coincides with our results, as cytokeratin constitutes an important intracellular anchorage of hemidesmosomes, which attach epithelial cells to the BM [Alberts et al., 2015]. Nakano et al. [2001] showed that most bovine TGCs in culture, which expressed uniform cytoplasmic staining of PL, did not show a staining of cytokeratin. Only a very small minority of the PL-positive TGCs showed a weak staining of cytokeratin. Despite the interpretation of Nakano et al. [2001] that PL-producing TGCs did not have any cytokeratin, it seems possible to us that this small minority of TGCs with simultaneous staining of PL and cytokeratin could correspond to TGCs found in our study showing contact to the BM as well as membrane-bound granules, even though, as soon as PL production starts, cytokeratin expression decreases. This indicates that TGC maturation and migration is associated with a reciprocal regulation of these proteins [Nakano et al., 2001]. Therefore, as cytokeratin also represents the intracellular part of desmosomes [Getsios et al., 2004; Coch and Leube, 2016], we interpret desmosome-possessing TGCs, which have been shown by Morgan and Wooding [1983], as being early stages of TGCs.

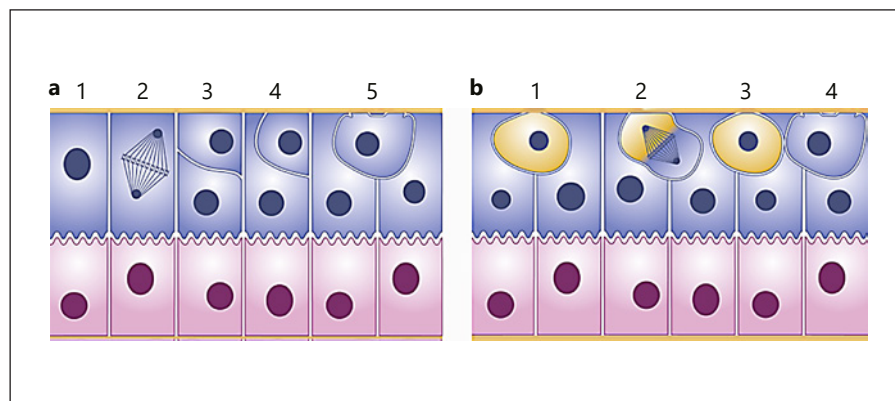
We observed an intracellular layer of electron-dense material underlying the cell membrane of some TGCs and in relation to the microvilli of UTCs. Based on the ultrastructural appearance and the fact that actin is a main component of the microvilli frame in other epithelial cells [Fath and Burgess, 1995; Coch and Leube, 2016],

we interpret this electron-dense material in both cell types as a part of the actin cytoskeleton. This interpretation is reinforced by immunogold [Lang et al., 2004] and immunohistochemical staining [Nakano et al., 2005]. Actin [Lang et al., 2004] as well as α_6 - and β_1 -integrin subunits and laminin [Pfarrer et al., 2003] have been suggested to be involved in TGC migration. As $\alpha_6\beta_1$ -integrin, also called VLA-6 (very late antigen-6) [Hemler et al., 1988], can interact indirectly with actin intracellularly [Alberts et al., 2015] and with laminin extracellularly [Sonnenberg et al., 1988; Alberts et al., 2015], the simultaneous staining of laminin and α_6 - and β_1 -integrin subunits along the cell membrane of TGCs lead to the interpretation that these proteins cooperate in TGC migration [Pfarrer et al., 2003]. Laminin and $\alpha_6\beta_1$ -integrin-dependent cell movement has also been described in epithelial cancer cells [Tani et al., 1997]. Another protein that might be involved in TGC migration is E-cadherin [Nakano et al., 2005]. Nakano et al. [2005] interpreted their findings of the redistribution of E-cadherin from the membrane-associated location to the cytoplasm in TGCs to play a role for TGC migration apically of tight junctions. Downregulation of membrane-associated E-cadherin has been described as an event during epithelial-mesenchymal transition (EMT) in other tissues [Morali et al., 2001; Yang and Liu, 2001]. EMT plays an important role in different biological processes, such as fetal development, tumor metastasis, and renal interstitial fibrosis [Yang and Liu, 2001; Thiery, 2002; Yang and Weinberg, 2008], as well as in the development of extravillous cytotrophoblast of the human placenta [Vicovac and Aplin, 1996; Davies et al., 2016]. Based on the above-mentioned findings of Nakano et al. [2005], EMT might also play a role in the development of bovine TGCs.

The presence of a BUC could be confirmed in all evaluated animals. Based on morphological characteristics, we assume that these BUCs are the precursors of TGCs. Since TGCs migrate from the basal part of the trophodermal epithelium towards the maternal tissue [Wathes and Wooding, 1980; Wooding and Wathes, 1980; Wooding, 1983], it appears obvious that their direct progenitor is located within the basal part of the epithelium. Furthermore, BUCs tend to have narrow contacts to the BM (Fig. 5b, c), assuming that these cells are in the process of losing contact to the BM, as it would be necessary for the development of TGCs. Additionally, a DLB, which has been described to be a characteristic structure of TGCs [Wooding and Burton, 2008], was shown in 2 BUCs.

According to Wooding and his colleagues [Wooding, 1992; Wooding and Burton, 2008], these BUCs would

Fig. 7. Schematic drawings of 2 potential modes of the formation of BUCs in the bovine trophoblast epithelium. The fetal trophoblast epithelium is drawn on top, with the maternal uterine epithelium below. **a** A typical UTC (1) undergoes an asymmetric mitosis (2) which leads to 2 different cells: 1 apically located cell and 1 BUC (3). This latter cell gradually reduces the contact to the BM (4 and 5). **b** A basally located stem cell (yellow cell; 1) is present in the trophoblast epithelium. This cell performs a self-renewing asymmetric mitosis (2), which leads to 1 stem cell (yellow cell; 3) and 1 BUC (4).



represent a transient cell between UTCs and TGCs. UTCs are morphologically and functionally distinct from TGCs [Igwebuike, 2006]. Consequently, such a development would be a transdifferentiation process, in which one differentiated cell undergoes a dedifferentiation into another specialized cell type [Rawlins and Hogan, 2006]. Differentiated cells have been shown to possess the ability for transdifferentiation in several other organs [Gordon and Lane, 1984; Michalopoulos et al., 2005].

In epithelial tissues that need continuous cell supply, proliferating cells can be separated into 2 groups: cells which show slow cycling activity, and cells which show fast cycling activity. The slowly cycling cells are interpreted to be the tissue-specific stem cells, which have the capability for self-renewal and give rise to cells of the second, fast cycling group. These fast cycling cells, the so-called transit-amplifying cells, have a reduced ability of self-renewal and arrange primarily supply to the sufficient number of specialized cells by progressive step-by-step differentiation and maturation [Lajtha, 1979; Potten and Loeffler, 1990; Tsujimura et al., 2002]. Transferred to the bovine trophoblast epithelium, it could be hypothesized that the UTCs, which show proliferative activity [Schuler et al., 2000], represent this “transit-amplifying” cell population and ensure the TGC ordnance by transdifferentiation. Findings of heterogeneous immunohistochemical staining of UTCs [Nishita et al., 1990] may reflect the step-by-step differentiation of these “transit-amplifying” cells. It remains open whether a slow cycling progenitor cell exists for the “transit-amplifying” UTCs.

Alternatively, it could be hypothesized that the BUCs represent a distinct stem cell population for the TGCs. Their basal localization within the trophoblast epithelium is reminiscent of epithelial stem cells in other tissues [Marei and Abd El-Gawad, 2001; Kurzrock et al., 2008]. Fur-

thermore, their ultrastructural appearance, which has been assessed subjectively, seems to represent a rather high nuclear-cytoplasmic ratio and spare rER and mitochondria. These properties bear resemblance to the basal progenitor cells of the respiratory tract [Marei and Abd El-Gawad, 2001]. Since we did not detect a Golgi apparatus in any of the BUCs, it is likely that these cells have only a small sized Golgi apparatus with low productivity. These observations raise the question as to whether BUCs could represent a cell population that differentiates into TGCs without having their origin in UTCs (Fig. 7b). As no sign for fast cycling cells between BUCs and TGCs have been observed, in this new theory, BUCs would differentiate directly into postmitotic TGCs without morphological different “transit-amplifying” cells. There remains the option that the BUC population itself can be divided in a slow cycling cell group and a “transit-amplifying” cell group. To verify this hypothesis, further investigations would be needed, for example the combination of staining with proliferation marker and three-dimensional imaging.

In conclusion, we have shown that there is a BUC type within the bovine trophoblast epithelium. The presence of such a cell type as an intermediate state between UTCs and TGCs has previously been postulated, but has never been revealed [Wooding, 1992; Wooding and Burton, 2008]. Based on morphological findings, we suggest, in accordance with Wooding and his colleagues [Wooding, 1992; Wooding and Burton, 2008], that BUCs are the progenitor cells of TGCs. To clarify the question of whether the BUCs themselves develop from UTCs [Wooding, 1992; Wooding and Burton, 2008], or if they are a separate self-replicating cell population (Fig. 7a, b), further investigation is needed.

Acknowledgements

The authors thank Miriam Lucas-Droste, Scientific Center for Optical and Electron Microscopy, ETH Zurich, for her guidance and the production of SBF-SEM images, and to Moritz Kirschmann, Center of Microscopy and Image Analysis, University of Zurich, for his support with the image processing and 3D-modelling. We are grateful to Elisabeth Hoegger and Elisabeth Schraner, Institute of Veterinary Anatomy, University of Zurich, for their technical advice and support with the light and electron microscopical imaging, and Lutz Slomianka, Institute of Anatomy, University of Zurich, for his guidance and support with stereology. We also thank Jeanne Peter, Vetcom, University of Zurich, for graphical illustrations.

Disclosure Statement

The authors declare no conflicts of interest.

References

- Alberts, B., A. Johnson, J. Lewis, M. Raff, K. Roberts, P. Walter (2015) *Molecular Biology of the Cell*, ed 6. New York, Garland Science.
- Björkmann, N.H. (1968) Fine structure of cryptal and trophoblastic giant cells in the bovine placenta. *J Ultrastruct Res* 24: 249–258.
- Björkmann, N.H. (1969) Light and electron microscopic studies on cellular alterations in the normal bovine placenta. *Anat Rec* 163: 17–30.
- Coch, R.A., R.E. Leube (2016) Intermediate filaments and polarization in the intestinal epithelium. *Cells* 5: E32.
- Davies, J.E., J. Pollheimer, H.E.J. Yong, M.I. Kokinos, B. Kalionis, M. Knofler, P. Murthi (2016) Epithelial-mesenchymal transition during extravillous trophoblast differentiation. *Cell Adhes Migr* 10: 310–321.
- Deerinck, T.J., E.A. Bushong, A. Thor, M.H. Ellisman (2010) NCMIR methods for 3D EM: a new protocol for preparation of biological specimens for serial block face scanning electron microscopy. National Center for Microscopy and Imaging Research. <https://ncmir.ucsd.edu/sbem-protocol> (accessed December 7, 2017).
- Fath, K.R., D.R. Burgess (1995) Microvillus assembly: not actin alone. *Curr Biol* 5: 591–593.
- Getsios, S., A.C. Huen, K.J. Green (2004) Working out the strength and flexibility of desmosomes. *Nat Rev Mol Cell Biol* 5: 271–281.
- Gordon, R.E., B.P. Lane (1984) Ciliated cell differentiation in regenerating rat tracheal epithelium. *Lung* 162: 233–243.
- Green, J.A., S.C. Xie, X. Quan, B.N. Bao, X.S. Gan, N. Mathialagan, J.F. Beckers, R.M. Roberts (2000) Pregnancy-associated bovine and ovine glycoproteins exhibit spatially and temporally distinct expression patterns during pregnancy. *Biol Reprod* 62: 1624–1631.
- Greenstein, J.S., R.W. Murray, R.C. Foley (1958) Observation on the morphogenesis and histochemistry of the bovine preattachment placenta between 16 and 33 days of gestation. *Anat Rec* 132: 321–341.
- Haeger, J.D., N. Hambruch, C. Pfarrer (2016) The bovine placenta in vivo and in vitro. *Theriogenology* 86: 306–312.
- Hemler, M.E., C. Crouse, Y. Takada, A. Sonnenberg (1988) Multiple very late antigen (VLA) heterodimers on platelets. Evidence for distinct VLA-2, VLA-5 (fibronectin receptor), and VLA-6 structures. *J Biol Chem* 263: 7660–7665.
- Hoffman, L.H., F.B.P. Wooding (1993) Giant and binucleate trophoblast cells of mammals. *J Exp Zool* 266: 559–577.
- Igwebuike, U.M. (2006) Trophoblast cells of ruminant placentas – a minireview. *Anim Reprod Sci* 93: 185–198.
- King, G.J., B.A. Atkinson, H.A. Robertson (1980) Development of the bovine placenta from days 20 to 29 of gestation. *J Reprod Fertil* 59: 95–100.
- Klisch, K., W. Hecht, C. Pfarrer, G. Schuler, B. Hoffmann, R. Leiser (1999a) DNA-content and ploidy level of bovine placental trophoblast giant cells. *Placenta* 20: 451–458.
- Klisch, K., R. Leiser (2003) In bovine binucleate trophoblast giant cells, pregnancy-associated glycoproteins and placental prolactin-related protein-1 are conjugated to asparagine-linked N-acetylgalactosaminyl glycans. *Histochem Cell Biol* 119: 211–217.
- Klisch, K., C. Pfarrer, G. Schuler, B. Hoffmann, R. Leiser (1999b) Tripolar acytokinetic mitosis and formation of feto-maternal syncytia in the bovine placenta: different modes of the generation of multinuclear cells. *Anat Embryol* 200: 229–237.
- Kurzrock, E.A., D.K. Lieu, L.A. Degraffenried, C.W. Chan, R.R. Isseroff (2008) Label-retaining cells of the bladder: candidate urothelial stem cells. *Am J Physiol Renal Physiol* 294: 1415–1421.
- Lajtha, L.G. (1979) Stem cell concepts. *Differentiation* 14: 23–33.
- Lang, C.Y., S. Hallack, R. Leiser, C. Pfarrer (2004) Cytoskeletal filaments and associated proteins during restricted trophoblast invasion in bovine placentas: light and transmission electron microscopy and RT-PCR. *Cell Tissue Res* 315: 339–348.
- Lee, C.S., M.M. Ralph, K.J. Gogolinewens, M.R. Brandon (1990) Monoclonal-antibody (Sbu-1 and Sbu-3) identification of cells dissociated from the sheep placental trophoblast. *J Histochem Cytochem* 38: 649–652.
- Marei, H.E.S., M.A. El-Gawad (2001) Differentiation of ciliated cells in the terminal bronchioles of neonatal calves. *Eur J Morphol* 39: 269–276.
- Mayhew, T.M. (1991) The new stereological methods for interpreting functional morphology from slices of cells and organs. *Exp Physiol* 76: 639–665.
- Michalopoulos, G.K., L. Barua, W.C. Bowen (2005) Transdifferentiation of rat hepatocytes into biliary cells after bile duct ligation and toxic biliary injury. *Hepatology* 41: 535–544.
- Morali, O.G., V. Delmas, R. Moore, C. Jeanney, J.P. Thiery, L. Larue (2001) IGF-II induces rapid β -catenin relocation to the nucleus during epithelium to mesenchyme transition. *Oncogene* 20: 4942–4950.
- Morgan, G., F.B.P. Wooding (1983) Cell migration in the ruminant placenta: a freeze-fracture study. *J Ultrastruct Res* 83: 148–160.
- Nakano, H., A. Shimada, K. Imai, T. Takahashi, K. Hashizume (2005) The cytoplasmic expression of E-cadherin and β -catenin in bovine trophoblasts during binucleate cell differentiation. *Placenta* 26: 393–401.
- Nakano, H., T. Takahashi, K. Imai, K. Hashizume (2001) Expression of placental lactogen and cytokeratin in bovine placental binucleate cells in culture. *Cell Tissue Res* 303: 263–270.
- Nishita, T., C. Kinoshita, M. Maegaki, M. Asari (1990) Immunohistochemical studies of the carbonic anhydrase isozymes in the bovine placenta. *Placenta* 11: 329–336.
- Pfarrer, C., P. Hirsch, M. Guillomot, R. Leiser (2003) Interaction of integrin receptors with extracellular matrix is involved in trophoblast giant cell migration in bovine placentas. *Placenta* 24: 588–597.
- Potten, C.S., M. Loeffler (1990) Stem cells: attributes, cycles, spirals, pitfalls and uncertainties. Lessons for and from the crypt. *Development* 110: 1001–1020.
- Rawlins, E.L., B.L. Hogan (2006) Epithelial stem cells of the lung: privileged few or opportunities for many? *Development* 133: 2455–2465.
- Schnorr, B., M. Kressin (2011) *Embryologie der Haustiere*. Stuttgart, Enke.

- Schuler, G., C. Wirth, K. Klisch, K. Failing, B. Hoffmann (2000) Characterization of proliferative activity in bovine placentomes between day 150 and parturition by quantitative immunohistochemical detection of ki67-antigen. *Reprod Dom Anim* 35: 157–162.
- Sonnenberg, A., P.W. Modderman, F. Hogervorst (1988) Laminin receptor on platelets is the integrin VLA-6. *Nature* 336: 487–489.
- Suzuki, R., T. Domon, M. Wakita, T. Akisaka (2003) The reaction of osteoclasts when releasing osteocytes from osteocytic lacunae in the bone during bone modeling. *Tissue Cell* 35: 189–197.
- Tani, T., A. Lumme, A. Linnala, E. Kivilaakso, T. Kiviluoto, R.E. Burgeson, L. Kangas, I. Leivo, I. Virtanen (1997) Pancreatic carcinomas deposit laminin-5, preferably adhere to laminin-5, and migrate on the newly deposited basement membrane. *Am J Pathol* 151: 1289–1302.
- Thiery, J.P. (2002) Epithelial-mesenchymal transitions in tumour progression. *Nat Rev Cancer* 2: 442–454.
- Touzard, E., P. Reinaud, O. Dubois, C. Guyader-Joly, P. Humblot, C. Ponsart, G. Charpigny (2013) Specific expression patterns and cell distribution of ancient and modern PAG in bovine placenta during pregnancy. *Reproduction* 146: 347–362.
- Tsujimura, A., Y. Koikawa, S. Salm, T. Takao, S. Coetzee, D. Moscatelli, E. Shapiro, H. Lepor, T.T. Sun, E.L. Wilson (2002) Proximal location of mouse prostate epithelial stem cells: a model of prostatic homeostasis. *J Cell Biol* 157: 1257–1265.
- Vicovac, L., J.D. Aplin (1996) Epithelial-mesenchymal transition during trophoblast differentiation. *Acta Anat* 156: 202–216.
- Wango, E.O., F.B.P. Wooding, R.B. Heap (1990) The role of trophoblastic binucleate cells in implantation in the goat: a morphological study. *J Anat* 171: 241–257.
- Wathes, D.C., F.B.P. Wooding (1980) An electron-microscopic study of implantation in the cow. *Am J Anat* 159: 285–306.
- Wimsatt, W.A. (1951) Observations on the morphogenesis, cytochemistry, and significance of the binucleate giant cells of the placenta of ruminants. *Am J Anat* 89: 233–281.
- Wooding, F.B. (1992) Current topic: the synepitheliochorial placenta of ruminants: binucleate cell fusions and hormone production. *Placenta* 13: 101–113.
- Wooding, F.B.P. (1983) Frequency and localization of binucleate cells in the placentomes of ruminants. *Placenta* 4: 527–540.
- Wooding, F.B.P., J.F. Beckers (1987) Trinucleate cells and the ultrastructural localisation of bovine placental lactogen. *Cell Tissue Res* 247: 667–673.
- Wooding, F.B.P., D.C. Wathes (1980) Binucleate cell migration in the bovine placenta. *J Reprod Fertil* 59: 425–430.
- Wooding, P., G.J. Burton (2008) *Comparative Placentation Structures, Functions and Evolution*. Berlin, Springer.
- Yang, J., Y. Liu (2001) Dissection of key events in tubular epithelial to myofibroblast transition and its implications in renal interstitial fibrosis. *Am J Pathol* 159: 1465–1475.
- Yang, J., R.A. Weinberg (2008) Epithelial-mesenchymal transition: at the crossroads of development and tumor metastasis. *Dev Cell* 14: 818–829.
- Zoli, A.P., P. Demez, J.-F. Beckers, M. Reznik, A. Beckers (1992) Light and electron microscopic immunolocalization of bovine pregnancy-associated glycoprotein in the bovine placenta. *Biol Reprod* 46: 623–629.